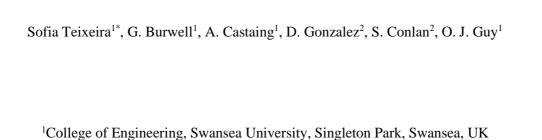




Cronfa - Swansea University Open Access Repository
This is an author produced version of a paper published in : Sensors and Actuators B: Chemical
Cronfa URL for this paper:
http://cronfa.swan.ac.uk/Record/cronfa28115
Paper: Teixeira, S., Burwell, G., Castaing, A., Gonzalez, D., Conlan, R. & Guy, O. (2014). Epitaxial graphene immunosensor for human chorionic gonadotropin. <i>Sensors and Actuators B: Chemical, 190</i> , 723-729.
http://dx.doi.org/10.1016/j.snb.2013.09.019

This article is brought to you by Swansea University. Any person downloading material is agreeing to abide by the terms of the repository licence. Authors are personally responsible for adhering to publisher restrictions or conditions. When uploading content they are required to comply with their publisher agreement and the SHERPA RoMEO database to judge whether or not it is copyright safe to add this version of the paper to this repository. http://www.swansea.ac.uk/iss/researchsupport/cronfa-support/

Epitaxial graphene immunosensor for human chorionic gonadotropin



²College of Medicine, Swansea University, Singleton Park, Swansea, UK

*To whom correspondence should be addressed. College of Engineering, Swansea University, Singleton Park, SA2 8PP, Swansea, UK. E-mail address: 607010@swansea.ac.uk; Tel: +44 01792602816.

Abstract

Human chorionic gonadotropin (hCG), a 37 kDa glycoprotein hormone, is a key diagnostic marker of pregnancy and has been cited as an important biomarker in relation to cancerous tumors found in the prostate, ovaries and bladder.

A novel chemically-modified epitaxial graphene diagnostic sensor has been developed for ultrasensitive detection of the biomarker hCG. Multi-layer epitaxial graphene (MEG), grown on silicon carbide substrates, was patterned using electron beam lithography to produce channel based devices. The MEG channels have been amine terminated using 3-Aminopropyl-triethoxysilane (APTES) in order to attach the anti-hCG antibody to the channel.

Detection of binding of hCG with its graphene-bound antibody was monitored by measuring reduction of the channel current of the graphene biosensor. The sensitivity of the sensor device was investigated using varying concentrations of hCG, with changes in the channel resistance of the sensor observed upon exposure to hCG. The detection limit of the sensor was 0.62 ng/mL and the sensor showed a linear response to hCG in the range 0.62 to 5.62 ng/mL with a response of 142 Ω /ng/mL. At concentrations above 5.62 ng/mL the sensor begins to saturate.

Keywords

Epitaxial graphene, immunosensor, human chorionic gonadotropin, SiC, amperometric, APTES

1. Introduction

Electrochemical immunosensors offer a number of significant advantages, including high sensitivity, fast response, simplicity, and relatively low cost [1, 2] when compared with other types of immunosensor. These advantages make them attractive for high performance analytical detection of biomolecules [3]. Immunosensors capable of detecting nucleic acids [4], viruses [5], antigens [6], and hormone [7] biomarkers, based on silicon nanowire [5], carbon nanotube (CNT) [8], graphite [9] have been widely reported. Since the pioneering work on SiNW sensors by Lieber *et al* [10], SiNW sensors have been developed that are capable of detection limits down to fg ml⁻¹ concentrations – such as reported for prostate specific antigen (PSA) detection by Kim *et al* [11]. CNT sensors have also been used to achieve detection of antigens e.g. PSA at ng ml⁻¹ [8, 12]

More recently, graphene has been utilized in a number of forms for sensor and biosensor applications [13-17].

Graphene's electronic structure and high surface to volume ratio contribute to the high sensitivity of graphene sensor devices [18]. Various forms of graphene and related materials (such as exfoliated graphene [19], graphene oxide and epitaxial graphene [20]), have been reported for use in graphene-modified electrodes and graphene-composite electrodes. An electrochemical sensor, using chemically modified exfoliated graphene to detect dopamine (DA), was reported to have a detection limit of 0.01 µM. [21]. Li et al. reported a novel electrochemical immunosensor of the breast cancer marker protein CA 15-3 using a highly conductive graphene-modified electrode. This sensor was capable of sensitive and label-free detection with a detection limit of 0.012 IU/mL [19]. Yasuhide et al. reported a label-free immunosensor based on an aptamer-modified graphene field-effect transistor (G-FET). The aptamer-modified G-FET showed selective electrical detection of IgE protein with an dissociation constant of 47 nM, indicating good affinity and the potential for G-FETs to be used in biological sensors [15]. Srivastave et al. reported an easy method for producing functionalized multilayer graphene from multiwalled carbon nanotubes (MWCNTs) in mass scale using only concentrated H₂SO₄/HNO₃. This biosensor shows linearity of 10-100 mg dL⁻ ¹, sensitivity of 5.43 µA mg⁻¹ dL cm⁻², lower detection limit of 3.9 mg dL⁻¹, [22]. Lu et al. reported an hydrogen peroxide biosensor formed from single-layer graphene with a detection limit of 1.05x10⁻⁷ M [23]. Schedin et al. reported a sensor for detection of individual gas molecules adsorbed on graphene with a detection limit of 1 ppb [24].

Epitaxial growth on silicon carbide (SiC) is a widely used method of producing high quality graphene. Using insulating or semi-insulating SiC substrates enables the lithographic fabrication of graphene devices, for electronic applications without the need for transfer to other substrates [25, 26]. Graphene can be grown on both the silicon and carbon faces of 4H-SiC, but growth is substantially different on each face, in terms of the morphology and

electronic structure of the resulting graphene layers [27]. Silicon face growth yields an interfacial layer between the SiC substrate and graphene, and typically grows layer-by-layer [28]. In contrast, carbon face growth yields layers which are decoupled from the SiC substrate, without a noticeable interface effect [29]. Larger growth domains are produced on the carbon face, which contributes to higher carrier mobilities in a microchannel device [30]. Graphene biosensors can be fabricated by covalent immobilization, of proteins to graphene surfaces [31, 32]. Covalent immobilization of antibody molecules onto graphene requires a chemical reaction of the COOH functional groups of the antibody, with amine groups, bound to the graphene surface, producing a peptide bond. Methods for amine functionalization of graphene include diazotization [33], thiol chemistry [34] and surface silanization using APTES. APTES attachment can be performed on various substrates provided they contain surface hydroxyl groups, which can react with alkoxysilanes to form covalent Si-O-C bonds to the underlying substrate.

An epitaxial graphene immunosensor, capable of selectively detecting hCG, has been developed. Human chorionic gonadotropin (hCG) is a glycoprotein hormone composed of 244 amino acids with a molecular mass of 36.7 kDa, produced by normal trophoblast cells of the placenta during pregnancy [35]. Trophoblast cells form the outer layer of a blastocyst, which provide nutrients to the embryo and develop into a large part of the placenta. Trophoblasts are formed during the first stage of pregnancy and are the first cells to differentiate from the fertilized egg. hCG is also produced by trophoblast cells in hydatidiform moles and choriocarcinoma (trophoblast diseases) in patients with germ cell tumors (testicular choriocarcinoma, placental site tumors and germ cell carcinomas of the ovary) and sometimes in patients with other malignancies [35].

In this work, standard lithographic techniques have been used to pattern epitaxial graphene devices, whose dimensions are scalable and suitable for wafer scale production. Epitaxial graphene devices have been functionalized using APTES, the first reported use of APTES on epitaxial graphene devices, to achieve an amine-terminated graphene surface. Antibodies targeted against hCG have been bound to the amine-terminated graphene in the first reported amperometric immunosensor based on epitaxial graphene. Device fabrication and surface functionalisation methods are readily adaptable to other antibody/antigen systems, and are thus suitable as a generic immunosensor platform.

2. Experimental Section

2.1. Materials and Reagents

Semi-insulating 4H-SiC substrates (nominally on-axis) were purchased from CREE. Synthetic urine was prepared with urea, sodium chloride, potassium chloride and sodium

phosphate purchased from Sigma-Aldrich. N-Hydroxysuccinimide (NHS) and N-(3-Dimethylaminopropyl)-N-ethylcarbodiimide hydrochloride (EDAC), Di-tert-butyl dicarbonate (t-BOC), sodium bicarbonate, bovine serum albumin (BSA), phosphate buffered saline (PBS), Potassium hexacyanoferrate III (K₃[Fe(CN)₆]), potassium hexacyanoferrate II (K₄[Fe(CN)₆]) trihydrate, and trifluoroacetic acid were all purchased from Sigma-Aldrich. Electrochemical measurements of the surface modification were performed using an aqueous reference electrode (Ag/AgCl) purchased from IJ Cambria Scientific Ltd and platinum (Pt) auxiliary electrode from BASi. hCG protein was purchased from Abcam (UK). Anti-hCG antibody was supplied by Ig Innovations.

2.2. Apparatus

Graphene growth was performed in a Jipelec Rapid Thermal Processing SiC furnace fitted with a turbo molecular pump. An e-Line (Raith GmBH) electron beam lithography system was used to define the graphene channels and contacts of the sensor device. Plasma etching of the graphene device was performed in an Oxford Instruments PlasmaLab. Cyclic voltammetry measurements were performed using an EmStat² Palm Sens potentiostat with the graphene channel device as the working electrode, a Pt auxillary electrode and Ag/AgCl reference electrode. Electrical measurements were performed using a Semi Probe LA-150 probe station with a Keithley 2602A Source Meter. Micro-Raman measurements were performed using a Renishaw InVia system with a 100 mW 532 nm excitation laser with approximately 10 mW of power on the sample. X-ray photoelectron spectroscopy (XPS) measurements were performed in a VG ESCAlab MKII with an Al X-ray excitation source (Kα of 1486 eV).

2.3. Graphene growth and device fabrication

4H-SiC wafers were cut into 10x10 mm samples and cleaned using a standard RCA procedure. Samples were etched in HF immediately prior to furnace growth to remove the native oxide. Multilayer graphene (MLG) was grown on the C-face of 4H-SiC at 1650°C and a vacuum of 10⁻⁴ mbar.

Electron beam lithography (EBL) followed by oxygen plasma etching (50 sccm O2, 75 mTorr and 50 W RF power, 60 seconds) was used to pattern graphene channel devices. A second EBL exposure was used to define the sputtered Ti/Au metal contacts to the graphene device. A third EBL exposure was used to define a window in PMMA, thus exposing only the graphene channel and protecting the metal contacts and the SiC surface from any chemical exposure during surface modification steps.

2.4. Hydroxylation of surface

The surface of the graphene channel devices was modified using the Fenton reaction [36], yielding an –OH terminated graphene layer. Epitaxial graphene samples were immersed in a solution of hydrogen peroxide and iron (II) sulfate, maintained at pH 3 for 30 minutes. Since the reaction is strongly exothermic, the iron sulfate powder was added to the solution incrementally and allowed to settle before introducing the graphene sample.

Contact angle measurements taken before and after the –OH termination reaction showed that the graphene surface changed from hydrophobic (90°) to hydrophilic (26°) following –OH termination.

2.5. Electrochemical assays

Cyclic Voltammetry (CV) measurements were conducted in 5.0 mmol/L of [Fe(CN)6]³⁻ and 5.0 mmol/L of [Fe(CN)6]⁴⁻, prepared in PBS buffer, pH 7.4. For CV assays, the potential was scanned from -0.7 V to +0.7 V, at 50 mV/s. All assays were conducted in triplicate.

2.6. Antibody immobilization with APTES

The –OH terminated graphene surfaces were reacted in a solution of 40% (3-Aminopropyl) triethoxysilane (APTES) in ethanol for 1.5 hours, to obtain an amine-terminated surface (Figure 1). Amine groups of the anti-hCG antibody were protected using Di-tert-butyl dicarbonate (t-BOC) to prevent cross-linking and aggregation of antibodies. This also ensures that only the amine-terminated surface of the graphene channel binds to the carboxylic group of the antibody.

The carboxylic groups of the antibody were activated using 50 mmol/L of N-(3-Dimethylaminopropyl)-N-ethylcarbodiimide hydrochloride (EDAC), and 25 mmol/L of N-hydrosucchimide (NHS). The EDAC generates an ester derivative of the antibody, which is subsequently stabilized by NHS in order to prevent it from undergoing hydrolysis and reverting back to the carboxylic acid. The ester derivative of anti-hCG subsequently reacts with the amine-terminated graphene surface, forming a peptide bond. The amine terminated graphene surface was exposed to a solution containing the activated antibodies for 2 hours at room temperature.

-Please insert Figure 1 here-

Removal of the t-BOC protecting groups, restoring the NH₂ groups on the antibody was achieved via cleavage of the amide bond between the t-BOC and the antibody using

trifluoroacetic acid (TFA) for 1 hour. This also hydrolyses the ester, generated by the activation of the carboxylic groups by EDAC and NHS, back into carboxylic groups. Bovine serum albumin (5% BSA in PBS) solution was subsequently applied for 10 minutes to the surface to block non-specific binding of the target hCG molecule to any free surface-amine groups.

2.7. hCG binding

hCG suspended in synthetic urine was applied at increasing concentrations, ranging from 3.1 mIU/mL to 28 mIU/mL (0.62 ng/mL to 5.62 ng/mL) to the graphene channel. Each concentration was applied to the surface for 15 minutes, followed by washing in PBS and drying in nitrogen.

3. Results and discussion

3.1. Characterization of graphene devices

The thickness of the graphene overlayer was estimated by curve fitting the C_{1s} core level peak from the XPS spectra of graphene grown on SiC, and differentiating the components of this peak related to the SiC substrate and the graphene layer respectively (Figure 2, c). Assuming the graphene growth follows a Franck van der Merwe growth or layer-by-layer mode, [37] the intensity of the SiC buried layer would decay exponentially with the increase in thickness of the graphene overlayer. This follows the propagation probability of the electrons through the solid [38], with the mean free path calculated as being 1.39 nm [39]; thus the graphene overlayer was estimated as being 3 layers thick.

Raman measurements on graphene channels, performed after lithographic fabrication steps, did not demonstrate any shifts due to contamination or damage to the graphene substrate. The position of the G peak in the Raman spectrum (1583 cm⁻¹), as well as the attenuation of the SiC substrate [40] were both used to determine the number of graphene layers, which was found to be in agreement with XPS results. The SiC background was subtracted from all Raman spectra to provide a clear comparison of the graphene peaks.

3.2. Characterization of surface modification

XPS was used to confirm the attachment of the aminosilane on the surface via the analysis of Si_{2p} , C_{1s} and N_{1s} peaks. Scans were performed with a pass energy of 10 eV. Curve fitting of the C_{1s} and Si_{2p} peaks was performed with a G/L ratio of 30%. The energy separation between the C_{1s} peak attributed to the SiC and the C_{1s} peak attributed to the graphene was kept

constant between the two experiments (before and after exposure to APTES), along with the FWHM of each peak.

Following APTES functionalization, the appearance of a nitrogen peak at 398.9 eV, consistent with an amine group, and of a secondary Si_{2p} peak at 101.4 eV (Figure 2, a and b), not present before functionalization, was observed. Taking into account the sensitivity factor of the different core levels, the contribution of both the nitrogen peak and the secondary silicon peak was found to be similar (Table 1), which is consistent with the 1:1 stoichiometric composition of the aminosilane. In addition, all the peaks shift by -0.1 eV, illustrating a Fermi shift, ergo a modification of the surface properties.

Curve fitting of the C_{1s} peak after exposure to APTES showed the appearance of a third C_{1s} peak (in addition to the bulk SiC and graphene C_{1s} peaks) attributed to the aliphatic carbon atoms of the APTES molecule (Figure 2, d). The contribution of these aliphatic carbon atoms to the XPS spectrum is just over 7 times that from the nitrogen or the silicon atoms of the APTES molecule. This is consistent with the stoichiometry expected when the APTES molecule (which should contain 9 carbon atoms) is bound to the graphene surface, after having lost an ethanol group, during the reaction with the hydroxyl-terminated surface. It was also observed that the intensity of the graphene peak decreased slightly, suggesting a modification of some of the sp^2 carbon atoms in the top most graphene layer to sp^3 hybridized carbon, due to the functionalization with hydroxyl groups.

-Please insert figure 2 here-

-Please insert Table1 here-

Chemical modification of graphene channels (the working electrode) can be measured by monitoring the changes in the electron transfer properties of the redox system [Fe(CN)6]^{3-/} [Fe(CN)6]⁴⁻ using cyclic voltammetry (CV). These studies are based on the assumption that the [Fe(CN)6]^{3-/4-} redox reaction is a simple, reversible electron transfer reaction. The ferri/ferrocyanide couple provides an ideal electrochemical probe for the study of chemically modified surfaces, since its reduction and oxidation both proceed via simple one electron transfer redox processes [41].

The obtained CV results from the hydroxyl-terminated graphene electrode before (control) and after modification with APTES are presented in Figure 3. The redox peak current of the control sample, corresponding to the oxidation potential of Fe(II), was at 464 mA. The peak current reduced to 110 mA for the APTES modified sample. This 354 mA shift of the redox peak indicates successful chemical modification of the surface with APTES as the formation

of the C-O-Si bond, between the graphene electrode and the APTES molecule, impedes the transfer of electrons between the electrode surface and the $[Fe(CN)6]^{3-/4-}$ electrolyte.

-Please insert figure 3 here-

Raman measurements were performed to monitor the effect of hydroxylation and APTES functionalization on the Raman spectrum of graphene (Figure 4). A notable increase in the D band intensity at ~1350 cm⁻¹ was measured, with the ratio of the D (sp³ bonded C) to G (sp² bonded C) Raman peaks, I(D)/I(G), increasing from ~0.08 to ~0.8 after –OH and APTES modification. This can be understood as an increase in sp³ hybridized carbon in the graphene layer, resulting from the functionalization reaction. This has been previously reported by [42], for the modification of exfoliated graphene with diazonium salts.

Raman mapping measurements were performed to assess any inhomogeneities in the APTES attachment. These mapping measurements of I(D)/I(G) indicated that APTES attached preferentially at the edges of the graphene channel, which may be caused by preferential hydroxylation of edge and defect sites during the Fenton reaction.

-Please insert figure 4 here-

3.3. Analytical performance of the sensor

Current-voltage characterisation of the graphene channel device was performed after each step of the surface modification process; from pristine graphene to anti-hCG attachment, to application of hCG. The initial APTES attachment showed an increase by a factor of 4 in the channel resistivity, which is to be expected considering that the covalent attachment to the surface induces a large amount of lattice defects (sp3 sites) into the graphene lattice, as evidenced by the Raman spectra in (Figure 4). These defect sites enhance the scattering of charge carriers, thus reducing carrier mobility [43].

Zeta potential measurements performed on the antibody in PBS solution at pH 7.4 yielded a potential of -6.14 mV.

Epitaxial graphene samples have been characterized as both n-type or p-type by different groups — depending on the growth conditions used [44]. In addition, the chemical functionalization of graphene may also influence the carrier type in graphene. The attachment of the negatively charged antibody is equivalent to a negative potential gating of the graphene channel, which if the graphene is n-type, would reduce the carrier density and thus the conductivity in the device. Analogous sensing mechanisms have been outlined in [45] for the

detection of negatively charged bacterial attachment to a p-type graphene-amine surface, whereby the hole current was increased by the negative gating potential.

This mechanism is therefore similar to that of a graphene chemFET. Defective graphene, and graphene influenced by extrinsic defects from the substrate is reported to be particularly sensitive to this potential gating effect [46], whereas pristine (defect-free) graphene is not strongly sensitive to this sensing mechanism. The presence of defects in graphene causes the current modulation from chemical gating to be enhanced, translating into superior sensitivity in chemFETS. Graphene grown on the C face of SiC is not a flat, uniform layer, but instead commonly grows into step-bunched terraces [47]. It is likely that structural defects from the epitaxial graphene growth, and chemical defects from the hydroxylation (Fenton) step, both contribute to the sensitivity of the current modulation from binding of the antibody.

Exposure of the antibody functionalized graphene sensor to the hCG antigen acts to increase the resistance across the channel. Indeed, increasing the concentration of hCG result in further increases in the graphene channel resistance, indicating that hCG was bound to the sensor. After exposure to concentrations above 5.62 ng/mL, the sensor response saturated, indicating that the active receptor sites had been occupied by the bound antigens.

As the SiC substrate is semi-insulating, applying a back gate is not feasible using these samples. $I-V_g$ measurements would be possible with a top or lateral gate, but this is beyond the scope of this work.

3.4. Sensitivity, selectivity and linearity of the sensor

Analysis of the biosensor response to hCG was carried out using varying concentrations of hCG in synthetic urine at pH 6.8. The sensor device (Figure 5), showed detectable changes in channel resistance upon exposure to hCG. The sensor had a linear response of $142 \Omega/ng/mL$ over the concentration range (0.62 to 5.62 ng/mL) with a limit of detection (LOD) of 0.62 ng/mL (3.1 mIU/mL). This range was chosen because the normal urinary concentration range of hCG in pregnant women is 5 mIU/mL to 117000 mIU/mL in clinical samples [48]). The graphene biosensor is thus more than sufficiently sensitive to detect the lower limit of hCG in clinical samples. For comparison, Manlan Tao *et al.* reported an hCG immunosensor with a LOD of 12 mIU/mL, which is linear in the range 25 to 400 mIU/mL [49].

Optimization of the sensor or use of multiple sensors would be required in order to span the relevant clinical concentration range. This can be achieved by varying the device geometry. Synthetic urine, with no hCG analyte induced a small amperometric change in the device, probably due to the electrolytic gating effect.

The unmodified graphene device had a two-terminal resistance of 62 Ω . This has no measurable response to hCG. After antibody attachment, the channel resistance increased by

16% on exposure to synthetic urine media (Figure 5, inset bottom right). Exposure to the first concentration of hCG (3.1 mIU/mL) further increased the channel resistance by 43%. The final concentration of hCG (5.62 mIU/mL) increased the channel resistance by 68% relative to the value in media. After antibody attachment, urea and cortisol were exposed to the antibody-modified graphene channels to measure the sensor selectivity to hCG. A negligible response was measured (Figure 5, inset top left). The sensor response (measured resistance) to urea and cortisol both vary by less than 20 Ohms which within the experimental error margin of the sensor. This is well below the response measured for hCG, where the measured resistance increases by 620 Ohms over the same concentration range. This indicates that there is little if any non-specific binding from urea or cortisol and that hCG produces a clearly detectable and specific response in the sensor.

Figure 5 illustrates that the sensor response to hCG is linear and is indicative of repeatable behavior in identical graphene sensors.

-Please insert figure 5 here-

3.5. Comparison with ELISA

ELISA tests are a standard technique for detecting the presence of an antigen within a sample. The sandwich ELISA provides high specificity by capturing an antigen with a specific antibody immobilized on a solid surface. The antigen becomes immobilized and it can be detected by a second antigen specific antibody termed the detection antibody. Detection is accomplished by assessing the activity of a conjugated enzyme antibody, specific to the detection antibody, via incubation with a substrate to produce data detectable change, usually through a color change. The most crucial element of the detection strategy is a highly specific antibody-antigen interaction. A sandwich ELISA was developed using the sheep anti-hCG antibody as detection antibody to compare the sensitivity of an ELISA to that of the amperometric biosensor. The ELISA test was performed under the same conditions (temperature, primary antibody concentration) as used for the amperometric sensor. A detection limit of 78 mIU/mL (15.6 ng/mL) was obtained using the ELISA method – this is 30 times less sensitive than the amperometric graphene sensor.

4. Conclusions

APTES functionalization, for amine termination of epitaxial graphene in order to attach antibody bioreceptors, has been used in the fabrication of an amperometric immunosensor, capable of selectively detecting the hormone hCG. This epitaxial graphene biosensor device has been demonstrated to be capable of detecting hCG concentrations as low as 0.62 ng/mL,

30 times more sensitive than an ELISA test performed under the same conditions. Since the attachment mechanism uses non-specific sites of the antibody (i.e. carboxylic groups) to bond to the NH₂ terminated surface, this method could potentially be adapted to attach other antibodies for the detection of other biomarkers. Thus, the APTES-modified graphene channel devices offer an easily adaptable, generic sensing platform for detection of a range of target biomarkers.

Acknowledgements

This work is part-funded by the European Social Fund (ESF) through the European Union's Convergence programme administered by the Welsh Government, Knowledge Economy Skills Scholarships (KESS), EPSRC Project: EP/I00193X/1.The authors would also like to acknowledge IG innovations for supplying the anti-hCG antibodies.

Captions for figures

Figure 1. Covalent attachment of 3-aminopropyltriethoxysilane (APTES) to the hydroxylterminated graphene surface.

Figure 2. (a) XPS core level spectrum of the Si_{2p} peak of an epitaxial graphene sample (grown on SiC) before functionalization, in black measured data and in red fitted peak attributed to SiC (b) XPS core level spectrum of the Si_{2p} peak of an epitaxial graphene sample after functionalization, in black measured data, in red fitted peak attributed to SiC and in blue fitted peak attributed to the silicon atom of the APTES molecule (c) XPS core level spectrum of the C_{1s} peak of a graphene sample before functionalization, in black measured data, in red fitted SiC peak and in blue fitted epitaxial graphene peak (d) XPS core level spectrum of the C_{1s} peak of a graphene sample after functionalization, in black measured data, in blue fitted graphene peak, in red fitted SiC peak and in green fitted APTES peak.

Table 1. Description of bonds and atomic abundances calculated from the fitted components of the C_{1s} , Si_{2p} and N_{1s} core peaks from XPS measurement before and after functionalization with APTES.

Figure 3. Cyclic Voltammograms measurements before (black) and after (red) APTES attachment.

Figure 4. Raman spectrum of graphene before (red) and after (black) APTES functionalization.

Figure 5. hCG concentration as a function of the resistance across a 100μmx4mm graphene channel. Urea and cortisol concentration as a function of the resistance across the channel (inset, top left). The I-V characteristics are plotted (inset, bottom right) for the unmodified device (black curve), amine terminated graphene surface (red curve), and AB attachment (blue curve).

References

- 1. P. Erden, and E. Kılıç, *A review of enzymatic uric acid biosensors based on amperometric detection*. Talanta, 107 (2013) 312-323.
- 2. P. Bobby and R.D. Marco, *Impedance spectroscopy: Over 35 years of electrochemical sensor optimization*, Electrochimica Acta, 51 (2006) 6217-6229
- 3. Y. Wan, et al., *Development of electrochemical immunosensors towards point of care diagnostics*. Biosensors & bioelectronics 47C (2013) 1-11.
- 4. G. J. Zhang et al., *Highly sensitive and reversible silicon nanowire biosensor to study nuclear hormone receptor protein and response element DNA interactions.* Biosensors & bioelectronics 26(2) (2010) 365-370.
- 5. D. Shirale, et al., *Effect of (L:D) Aspect Ratio on Single Polypyrrole Nanowire FET Device*. The journal of physical chemistry. C, Nanomaterials and interfaces 114(31) (2010) 13375-13380.
- 6. Tian, L. and T. Heyduk, *Antigen peptide-based immunosensors for rapid detection of antibodies and antigens*. Analytical chemistry 81(13) (2009) 5218-5225.
- 7. M. G. María et al., Ultrasensitive detection of adrenocorticotropin hormone (ACTH) using disposable phenylboronic-modified electrochemical immunosensors. Biosensors and Bioelectronics 35 (2012) 82-86.
- 8. H.T.L. John, H. Sabahudin, and W. Dashan, *Multiwall Carbon Nanotube (MWCNT) Based Electrochemical Biosensors for Mediatorless Detection of Putrescine*.
 Electroanalysis 17 (2005) 47-53.
- 9. S.S Ordóñez and E. Fàbregas, New antibodies immobilization system into a graphite-polysulfone membrane for amperometric immunosensors. Biosensors and Bioelectronics 22(6) (2007) 965-972.
- 10. Y. Cui et al., *Nanowire nanosensors for highly sensitive and selective detection of biological and chemical species.* Science 293(5533) (2001) 1289-1292.
- 11. A. Kim, et al., *Ultrasensitive*, *label-free*, *and real-time immunodetection using silicon field-effect transistors*. Applied Physics Letters, 91(10) (2007) 103901.
- 12. J. Okuno et al., Label-free immunosensor for prostate-specific antigen based on single-walled carbon nanotube array-modified microelectrodes. Biosensors & bioelectronics 22(9-10) (2007) 2377-2381.
- 13. E. Zor, et al., An electrochemical biosensor based on human serum albumin/graphene oxide/3-aminopropyltriethoxysilane modified ITO electrode for the enantioselective discrimination of D- and L-tryptophan. Biosensors & bioelectronics, 42 (2013) 321-325.
- 14. K. Yu, Z. Bo, G. Lu, S. Mao, S. Cui, Y. Zhu, X. Chen, R.S. Ruoff and J. Chen, *Growth of carbon nanowalls at atmospheric pressure for one-step gas sensor fabrication.* Nanoscale research letters 6(202) (2011) 1-9.
- 15. Y. Ohno, K. Maehashi, and K. Matsumoto, *Label-free biosensors based on aptamer-modified graphene field-effect transistors*. Journal of the American Chemical Society, 132(51) (2010) 18012-18013.
- 16. M. Pumera, et al., *Graphene for electrochemical sensing and biosensing*. Trends in Analytical Chemistry, 29 (2010) 954-965.
- 17. S Mao et al., *Highly sensitive protein sensor based on thermally-reduced graphene oxide field-effect transistor.* Nano Research 4 (10) (2011) 921-930.
- 18. S. Yuyan et al., *Graphene Based Electrochemical Sensors and Biosensors: A Review.* Electroanalysis 22(10) (2010) 1027-1036.
- 19. Li, H., et al., Electrochemical immunosensor with N-doped graphene-modified electrode for label-free detection of the breast cancer biomarker CA 15-3. Biosensors & bioelectronics 43 (2013) 25-29.
- 20. O.J. Guy, G. Burwell, Z. Tehrani, A. Castaing, K.A. Walker, S.H. Doak, Materials Science Forum, 711 (2012) 246-249.
- 21. T. Kuila et al., *Recent advances in graphene-based biosensors*. Biosensors & bioelectronics 26(12) (2011) 4637-4648.

- 22. R. Srivastava et al., Functionalized multilayered graphene platform for urea sensor. ACS nano 6(1) (2012) 168-175.
- 23. Q. Lu et al., Direct electrochemistry-based hydrogen peroxide biosensor formed from single-layer graphene nanoplatelet-enzyme composite film. Talanta 82(4) (2010) 1344-1348.
- 24. F. Schedin, A.K. Geim, S.V. Morozov, E.W. Hill, P. Blake, M.I. Katsnelson, K. S. Novoselov, *Detection of individual gas molecules adsorbed on graphene*. Nature Materials 6(9) (2007) 652-655.
- 25. A.E. Moutaouakil et al., *Room Temperature Logic Inverter on Epitaxial Graphene-on-Silicon Device*. Japanese Journal of Applied Physics 50(7) (2011) 113.
- 26. Kang, H.C., Karasawa, H., Miyamoto, Y., Handa, H., Suemitsu, T., Suemitsu, M., & Otsuji, T., *Epitaxial graphene field-effect transistors on silicon substrates*. Solid-State Electronics (2010). 54: p. 1010-1014.
- 27. J. Kedzierski, P.L. Hsu, P. Healey, P.W. Wyatt, C.L. Keast, M. Sprinkle, C. Berger, & W.A. de Heer, *Epitaxial graphene transistors on SiC substrates*. Electron Devices, IEEE Transactions 55(8), (2008) 2078-2085.
- 28. N. Srivastava, G. He, R.M. Feenstra, & P. Fisher, *Comparison of graphene formation on C-face and Si-face SiC surfaces*. Physical Review B 82(23) (2010) 235406.
- 29. N. Srivastava, G. He, P.C. Mende, R.M. Feenstra, Y. Sun, *Graphene formed on SiC under various environments: Comparison of Si-face and C-face.* Journal of Physics D: Applied Physics, 45 (2012) 154001.
- 30. J.A. Robinson, M. Wetherington, J.L. Tedesco, P.M. Campbell, X. Weng, J. Stitt, M.A. Fanton, E. Frantz, D. Snyder, B.L.VanMil, *Correlating Raman spectral signatures with carrier mobility in epitaxial graphene: A guide to achieving high mobility on the wafer scale.* Nano letters 9(8) (2009) 2873-2876.
- 31. C. Halliwell and A. Cass, A factorial analysis of silanization conditions for the immobilization of oligonucleotides on glass surfaces. Analytical chemistry 73(11) (2001) 2476-2483.
- 32. S. Steingrimur, H.K. Hena, and A.S Nate, *Targeting Antibodies to Carbon Nanotube Field Effect Transistors by Pyrene Hydrazide Modification of Heavy Chain Carbohydrates.* Journal of Nanotechnology, (2012). 2012.
- 33. E. Bekyarova et al., *Chemical modification of epitaxial graphene: spontaneous grafting of aryl groups.* Journal of the American Chemical Society 131(4) (2009) 1336-1337.
- 34. A. Bindoli, J. Fukuto, and H. Forman, *Thiol chemistry in peroxidase catalysis and redox signaling*. Antioxidants & redox signaling 10(9) (2008) 1549-1564.
- 35. M. Aizawa, et al., Enzyme immunosensor. III. Amperometric determination of human chorionic gonadotropin by membrane-bound antibody. Analytical biochemistry, 94(1) (1979) 22-28.
- 36. R.H. Bradley et al., *Surface studies of hydroxylated multi-wall carbon nanotubes*. Applied Surface Science 258 (2012) 4835-4843.
- 37. E. Bauer, *Phänomenologische Theorie der Kristallabscheidung an Oberflächen. II.* Zeitschrift für Kristallographie, (1958).
- 38. S. Kono, C.S. BFadley, N.F.T. Hall, Z. Hussain, *Azimuthal Anisotropy in Core-Level X-Ray Photoemission from c* (2× 2) *Oxygen on Cu* (001): *Experiment and Single-Scattering Theory*. Physical review letters 41(2) (1978) 117.
- 39. M.P. Seah, and W.A. Dench, *Quantitative electron spectroscopy of surfaces: A standard data base for electron inelastic mean free paths in solids.* Surface and Interface Analysis 1(1) (1979) 2-11.
- 40. D. Lee et al., Raman spectra of epitaxial graphene on SiC and of epitaxial graphene transferred to SiO2. Nano letters 8(12) (2008) 4320-4325.
- 41. S.D. Collyer, F. Davis, A. Lucke, J.M.C. Stirling and S.P.J. Higson, *The Electrochemistry of the Ferri/Ferrocyanide couple at a Calix[4] resorcinarenetetrathiol modified Gold Electrode as a study of novel*

- electrode modifying coatings for use within Electro-analytical Sensors. Journal of Electroanalytical Chemistry 549 (2003) 119-127.
- 42. P. Huang, H. Zhu, L. Jing, Y. Zhao & X. Gao, *Graphene covalently binding aryl groups: conductivity increases rather than decreases.* ACS nano 5 (2011) 7945-7949.
- 43. W.A. Heer, C. Berger, X. Wu, M. Sprinkle, Y. Hu, M. Ruan, J.A. Stroscio *Epitaxial graphene electronic structure and transport*. Journal of Physics D: Applied Physics, 43 (2010) 374007.
- 44. N. Mohanty, and V. Berry, *Graphene-Based Single-Bacterium Resolution Biodevice* and DNA Transistor: Interfacing Graphene Derivatives with Nanoscale and Microscale Biocomponents. Nano letters 8 (2008) 4469-4476.
- 45. B. Kumar, M. Kyoungmin, M. Bashirzadeh, A.B. Farimani, M.H. Bae, D. Estrada, Y.D. Kim, P. Yasaei, Y.D. Park, E. Pop, N.R. Aluru, A. Salehi-Khojin, *The role of external defects in chemical sensing of graphene field-effect transistors*. Nano Lett, 13(5) (2013) 1962-1968.
- 46. N. Camara, A. Tiberj, B. Jouault, A. Caboni, B. Jabakhanji, N. Mestres, P. Godignon, & J. Camassel, *Current status of self-organized epitaxial graphene ribbons on the C face of 6H--SiC substrates*. journal of Physics D: Applied Physics 43 (2010) 374011.
- 47. N. Camera, et al., Current status of self-organized epitaxial graphene ribbons on the C face of 6H–SiC substrates. Journal of Physics D: Applied Physics 43 (2010) 374011.
- 48. Peters, A., *The Diagnosis of Pregnancy*. Glob. libr. women's med., 2008.
- 49. M. Tao et al., *The preparation of label-free electrochemical immunosensor based on the Pt-Au alloy nanotube array for detection of human chorionic gonadotrophin.* Clinica chimica acta; international journal of clinical chemistry 412(7-8) (2011) 550-555.